Published in final edited form as:
J Neurosci. 2011 October 12; 31(41): 14735–14744. doi:10.1523/JNEUROSCI.1502-11.2011.

The anterior insular cortex represents breaches of taste identity expectation

Maria G. Veldhuizen[1,2], **Danielle Douglas**[1], **Katja Aschenbrenner**[1,2], **Darren R. Gitelman**, and **Dana M. Small**[*,1,2,3,4]

[1]Affective Sensory Neuroscience Laboratory, The John B. Pierce Laboratory, New Haven, CT 06519

[2]Department of Psychiatry, Yale University School of Medicine, New Haven, CT 06510

[3]Interdepartmental Neuroscience, Yale University School of Medicine, New Haven, CT 06510

[4]Department of Psychology, Yale University, New Haven, CT 06520

Abstract

Despite the importance of breaches of taste identity expectation for survival, its neural correlate is unknown. We used fMRI in 16 women to examine brain response to expected and unexpected receipt of sweet taste and tasteless/odorless solutions. During expected trials (70%) subjects heard "sweet" or "tasteless" and received the liquid indicated by the cue. During unexpected trials (30%) subjects heard "sweet" but received tasteless or they heard "tasteless" but received sweet. Following delivery, subjects indicated stimulus identity by pressing a button. Reaction time was faster and more accurate following valid cuing, indicating that the cues altered expectancy as intended. Tasting unexpected vs. expected stimuli resulted in greater deactivation in fusiform gyri, possibly reflecting greater suppression of visual object regions when orienting to, and identifying, an unexpected taste. Significantly greater activation to unexpected vs. expected stimuli occurred in areas related to taste (thalamus, anterior insula), reward (VS, OFC), and attention (anterior cingulate cortex, inferior frontal gyrus, IPS). We also observed an interaction between stimulus and expectation in the anterior insula primary taste cortex. Here response was greater for unexpected vs. expected sweet compared to unexpected vs. expected tasteless, indicating that this region is preferentially sensitive to breaches of taste expectation. Connectivity analyses confirmed that expectation enhanced network interactions, with IPS and VS influencing insular responses. We conclude that unexpected oral stimulation results in suppression of visual cortex and up-regulation of sensory, attention, and reward regions to support orientation, identification and learning about salient stimuli.

Introduction

Foods and drinks are generally identified by sight and smell before the decision to ingest is made. Consequently, we have a pretty good idea of what we expect to taste before doing so. Breaches of these taste expectations can then be very jarring, even if the unexpected sensation is rewarding under other circumstances. For example, one can imagine accidentally sipping a fine Chardonnay while expecting water. The sensation of the wine would be surprising and likely lead to the immediate halting of ingestion. Such a response, though negating the chance to savor fine Chardonnay, makes evolutionary sense since incorrect decisions to swallow can incur dire consequences.

Correspondence should be addressed to: Dana Small, The John B. Pierce Laboratory, 290 Congress Avenue, New Haven, CT, 06519. dsmall@jbpierce.org.

Despite the importance of breaches of taste identity expectation for survival, its neural correlate is unknown. Several lines of evidence suggest the insular cortex should be involved. The anterior insula houses primary taste cortex and plays an important role in taste quality coding (Scott and Plata-Salaman, 1999; Katz et al., 2002; Accolla et al., 2007). Insular taste responses are also sensitive to expectation (Nitschke et al., 2006). A bitter stimulus is rated as less intense and produces less response when subjects expect that it corresponds to the weaker compared to the stronger of two bitter stimuli (Nitschke et al., 2006). Manipulating beliefs by providing information about more abstract attributes, such as price (Plassmann et al., 2008) or brand (McClure et al., 2004), affect medial OFC rather than insular cortex. However, in all of these examples beliefs are manipulated and perception changes to align with expectation rather than to create a breach of expectation.

Although breaches of taste identity expectation have not been studied, breaches of taste temporal expectancy have been employed to study reward learning. Pavlovian prediction learning is mediated by the difference between what is expected and what is received (Rescorla and Wagner, 1972; Wagner and Rescorla, 1972). A positive error signal is generated if the stimulus is greater, and a negative error signal is generated if the outcome is less than expected. Breaches of taste *temporal* expectancy, thought to reflect error signaling, influence responses in the VS and OFC, but not insula (Berns et al., 2001; Pagnoni et al., 2002; McClure et al., 2003; O'Doherty et al., 2003; O'Doherty et al., 2006). Although the emphasis is on reward learning in these studies, breaches of expectation should generate not only an error signal, but also attentional reorienting, especially if the subject is engaged in a goal directed behavior (Maunsell, 2004).

Here we set out to determine the neural correlates of breaches of taste identity expectations with fMRI. Subjects received sweet and tasteless solutions that were either preceded by valid or invalid verbal cues. We predicted enhanced response to unexpected compared to expected taste in insular taste cortex. We also hypothesized that breaches of taste identity expectation would recruit attentional and reward networks reflecting attentional deployment and generation of error signals, and that these signals would serve to drive insular taste responses and thereby enhance processing of unexpected taste.

Material and Methods

Subjects

Twenty-two female (also taking part in a larger study looking at menstrual cycle), right-handed, non-smoking subjects (age: mean ± standard deviation: 25.4 ± 6.1 years) with a mean Edinburgh Handedness Inventory score of 81 ± 16.7 (Oldfield, 1971) were recruited through advertisements around Yale University and the city of New Haven. Subjects had an average body mass index (BMI) of 25.2 ± 5.5 kg/m^2 with a range of 19.1 – 38.7. All volunteers gave informed consent to participate in our study that was approved by the Yale University School of Medicine Human Investigation Committee. Subjects were excluded if they had a known taste, smell, neurological, psychiatric, or other pathological disorder. Two of the original subjects were excluded due to excessive movement during scanning (exceeding 1 mm of movement in any direction in more than one out of four runs) leaving 20 datasets for analyses (including 3 subjects that had one out of four runs excluded due to excessive movement). Another four subjects were excluded based on poor performance of the detection task during scanning (described below). The remaining sixteen female subjects were 25.1 ± 6.4 years old and had a mean Edinburgh Handedness inventory score of 80.6 ± 16.4. The average BMI was 24.9 ± 5.7.

Taste Stimuli and Delivery

The taste stimuli included a sweet sucrose solution (0.56 M) and a tasteless and odorless solution designed to mimic the ionic components of saliva (O'Doherty et al., 2001). We use the tasteless solution as the control stimulus since water activates taste cortex (Frey and Petrides, 1999; Zald and Pardo, 2000) and has a taste (Bartoshuk et al., 1964). Subjects were presented with four versions of the tasteless solution (2.5 mM sodium bicarbonate and 25mM potassium chloride, plus three dilutions at 25%, 50%, and 75% of the original concentration) and asked to select the one that tasted most like nothing.

A custom-designed gustometer was used to deliver the liquid stimuli as 0.5 mls of solution over 3s. This system has been successfully used in past fMRI studies (Veldhuizen et al., 2007; Small et al., 2008; Bender et al., 2009; Felsted et al., 2010). It consists of programmable syringe pumps holding syringes filled with taste solutions, connected to beverage tubes that pass from the control room to the scanner room and anchor into an fMRI-compatible custom-designed gustatory manifold mounted on the MRI headcoil. Separate tubes anchor into separate channels within the manifold that converge over a plastic stylus at the bottom of the manifold. The subject's tongue rests under the stylus and when the pump is triggered the liquid bolus drips onto the end of the stylus and rolls off the surface to the tongue.

Experimental Design

Subjects first participated in a stimulus selection and fMRI training session. This session served to select an appropriate tasteless solution, familiarize subjects with the task, and to identify subjects who found it uncomfortable to perform our task in a simulated fMRI environment.

Stimulus delivery occurred according to our long-event-related design depicted in detail in Figure 1A (Small et al., 2003; Small et al., 2004). Subjects were instructed to hold the stimulus in their mouth until cued to swallow by a tone and to indicate whether or not a taste was present by pressing a button. Half of the subjects were instructed to press a button with their right hand when they detected the sucrose solution and another button with their left hand when they detected a tasteless solution. The other half of the subjects received instructions for the reversed hand-response assignment.

The fMRI paradigm conformed to a 2 × 2 factorial design with expectation (expected vs. unexpected) and stimulus (tasteless or 0.56 M sucrose solution) as within-subject factors. During expected trials (70%) subjects heard either "sweet" or "tasteless" and received the liquid indicated by the verbal cue (ExpSwt or ExpTless). During unexpected trials (30%) subjects heard "sweet" but received tasteless (UnTless) or they heard "tasteless" but received sweet (UnSwt) (Figure 1B).

During the fMRI training session subjects underwent a single run in which all trials were valid. During actual scanning (on a separate day) subjects received both valid and invalid cues over four runs (each 712 seconds long and containing 35 events). There were 98 valid events (49 ExpSwt, 49 ExpTless) and 42 invalid events (21 UnSwt, 21 UnTless) across the four runs.

Subjects provided perceptual ratings of the stimuli before and after scanning. Pleasantness, edibility, wanting and familiarity were rated using visual analogue scales ('How pleasant is this taste?': "Most unpleasant sensation ever" = −100 mm, "Neutral" = 0, "Most pleasant sensation ever" = +100 mm), 'How edible is this taste?' ("Not edible at all" = −100 mm, "Neutral" = 0, "Very edible" = +100 mm), 'How much do you want to eat more of this?' ("I would never want to eat this"= −100 mm, "Neutral" = 0, "I would want to eat this more than

anything" = +100 mm), 'How familiar is this taste?' ("Not familiar at all" = −100 mm, "Neutral" = 0, "Very familiar" = +100 mm). The intensity, sweetness, saltiness, sourness and bitterness of the stimuli were evaluated on a cross-modal general Labeled Magnitude Scale (gLMS) (Green et al., 1996; Bartoshuk et al., 2006). This is a vertical line-scale of 100 mm with the label "barely detectable" at the lower anchor, and the label "strongest imaginable sensation" at the upper anchor. In between these labels the following words were approximately logarithmically spaced: "weak" (6 mm), "moderate" (17mm), "strong" (35 mm), and "very strong" (53 mm).

FMRI Scanner

Images were acquired on a Siemens 3 T Trio scanner. Echo planar imaging was used to measure the blood oxygenation-level dependent (BOLD) signal as an indication of cerebral brain activation. A susceptibility-weighted single-shot echo planar method was used to image the regional distribution of the BOLD signal with parameters of: TR: 2000ms; TE: 20 ms; flip angle: 90°; FOV: 220 mm; matrix: 64 × 64; slice thickness: 3 mm, and number of slices: 40. Slices were acquired in an interleaved mode to reduce the crosstalk of the slice selection pulse. At the beginning of each functional run, the MR signal was allowed to equilibrate over six scans ("dummy images") for a total of 12 s, which were then excluded from analysis. The anatomical scan used a T1-weighted 3D FLASH sequence (TR/TE: 2530/3.66 ms; flip angle: 20°; FOV: 256; matrix: 256 × 256; slice thickness: 1 mm; number of slices: 176).

FMRI Analysis

Data were analyzed on Linux workstations using Matlab (MathWorks, Inc., Sherborn, MA) and SPM5 (Wellcome Trust Centre for Neuroimaging, London, UK). Functional images were slice-time acquisition corrected using sinc interpolation to the slice obtained at 50% of the TR. All functional images were then realigned to the scan immediately preceding the anatomical T1 image. The images (anatomical and functional) were then normalized to the Montreal Neurological Institute template of grey matter, which approximates the anatomical space delineated by Talairach and Tournoux (Talairach and Tournoux, 1998). Images were then detrended, using a method for removing at each voxel any linear component matching the global signal (Macey et al., 2004). Functional images were smoothed with a 6 mm FWHM isotropic Gaussian kernel. For the time-series analysis on all subjects, a high pass filter (128 secs) was included in the filtering matrix (according to the convention in SPM5) in order to remove low-frequency noise and slow drifts in the signal. Condition-specific effects at each voxel were estimated using the general linear model. The response to events was modeled by a canonical hemodynamic response function (HRF) included in SPM5. The temporal derivative of the hemodynamic response function was also included as part of the basis set to account for up to 1-sec shifts in timing of the events (Henson et al., 2002). The events of interest were the four possible combinations of cue and stimulus (ExpSwt, ExpTless, UnSwt, UnTless), modeled as 3-sec mini-blocks (Figure 1A). Cues and swallows were modeled as nuisance effects. No head movement regressors were included, as subjects with head movements beyond 1 mm were excluded from the analysis. Parameter estimate images from each subject, and for each of the four event types were entered into a second level analysis using full factorial ANOVA with expectation (expected or unexpected) and stimulus (tasteless or 0.56M sucrose solution) as the two factors. T-maps of contrasts were thresholded for display at $P_{uncorrected} = 0.001$, with a cluster size threshold of 3 voxels.

Voxels were considered significant at $p < 0.05$ corrected for multiple comparisons using the false discovery rate (FDR) across the whole brain for unpredicted peaks and across small volumes defined using co-ordinates from prior studies as the centroid of a 6 mm sphere for predicted peaks. We predicted greater response in the anterior insula for unexpected oral

stimuli and used the peaks identified in Veldhuizen et al. (2007; 2011) and Bender et al. (2009) as centroids for volumes of interest. We also expected greater responses in the VS (McClure et al., 2003) and OFC for unexpected stimuli and used the peaks from McClure et al. (2003) and O'Doherty et al. (2003) to define these small volumes.

To examine expectancy-dependent changes in connectivity, we used psychophysiological interaction (PPI) analysis (Friston et al., 1997; Gitelman et al., 2003). Regions that showed a main effect of unexpected vs. expected at the group level were used as seed regions. The first eigenvariate of the time-series data was extracted from a 6 mm sphere with a centroid of each subjects' peak voxel. Subject specific peak voxels were determined by searching each individual subject's contrast of [UnSwt + UnTless] − [ExpSwt + ExpTless] (displayed at $p < 0.1$) for a peak within 6 mm of the group activation maxima shown in Table 2. The eigenvariate was then deconvolved (Gitelman et al., 2003), multiplied with the psychological variable (unexpected – expected) and reconvolved with a hemodynamic response function to form the psychophysiological interaction term. For each subject we computed new PPI parameter estimate images with the interaction as a regressor-of-interest, and the time-series eigenvariate and psychological variable as nuisance regressors. These images were then entered into a one-way ANOVA group analysis to examine which areas display increased connectivity with the seed regions under the unexpected condition compared to the expected condition. To isolate areas that also showed a main effect of unexpected-expected (from the main analysis described above), we saved a mask from the main analysis (thresholded at $P_{uncorrected} = 0.001$, with a cluster size threshold of 3 voxels). We then used this image as an inclusive mask in the PPI group analysis. T-maps were thresholded for display at $P_{uncorrected} = 0.001$, with a cluster size threshold of 3 voxels. Peaks were considered significant at $p < 0.05$ FDR corrected across voxels in the inclusive mask.

Finally, we used the dynamic causal modeling (DCM version 10) tool in SPM8 (Wellcome Trust Centre for Neuroimaging, London, UK) to determine whether responses in the most significantly activated reward (VS) and attentional (IPS) regions modulate sensory cortex in parallel or independently (Friston et al., 2003). As opposed to PPI, which only examines the connectivity from single source regions, DCM allows the examination and comparison of multiple network models containing multiple prespecified source regions. DCM requires the specification of intrinsic connectivity between the chosen regions (i.e., "steady state" connectivity) and driving inputs into at least one region in order to cause network activity. Additional modulatory inputs affect the strength of the intrinsic coupling in a context sensitive manner. Models were compared using Bayesian Model Selection (Stephan et al., 2009; Penny et al., 2010). Further details of the DCM models and model comparison are specified below.

Results

Behavioral

Perceptual Ratings—Perceptual ratings taken before and after training and before and after scanning were analyzed. Due to technical difficulties, we could not collect data for one subject, leaving a total of 15 datasets for perceptual analysis. We performed a 2 (stimulus: sweet vs. tasteless) × 2 (session: training vs. scan) × 2 (time: before vs. after session) within-subjects MANOVA on pleasantness, intensity, sweetness, sourness, saltiness, bitterness, edibility, familiarity and wanting ratings in SPSS for Windows (release 16.0.0, Chicago, SPSS Inc) in which we evaluated whether these characteristics differed across the stimuli, session, and time. We used an alpha of 0.05 to determine significance of each factor on the perceptual ratings. We report significant multivariate and univariate effects only. Post-hoc t-tests were used to further probe significant interaction effects.

We observed a significant multivariate effect for the taste factor ($F(9,6) = 10.558$, $p = 0.005$). Inspection of the univariate effects for this factor showed that the sweet stimulus was experienced as more intense ($F(1,14) = 45.456$, $p < 0.001$) and sweet ($F(1,14) = 66.746$, $p < 0.001$), and trended towards being more pleasant ($F(1,14) = 3.23$; $p = 0.094$) and edible ($F(1,14) = 3.99$, $p = 0.066$) than the tasteless stimulus (Figure 2). We observed a main effect of time on edibility ratings ($F(1,14) = 14.574$, $p = 0.002$) with both stimuli rated as less edible after the sessions. We also observed a significant interaction of time and session on wanting ratings ($F(1,14) = 8.060$, $p = 0.013$), such that before the scanning session the solutions were wanted more than after the scanning session ($p = 0.015$). No other main or interaction effects were observed. The results from this analysis suggest that perception was similar when all trials were valid (training run) compared to when expectation was occasionally breached (no effects of session). We did not collect perceptual ratings during training or scanning because perceptual evaluation influences brain response to taste (Bender et al., 2009) and we wanted to keep our subjects focused on the target detection task. Therefore we do not have data on the influence of expectation on perception. Rather, task performance was evaluated by analyzing reaction times and accuracy.

Detection Task Performance—Detection speed and accuracy were assessed for the four different events during the fMRI scan. Response time was defined as the time in milliseconds (ms) that elapsed between the arrival of the stimulus at the outflow point of the mouthpiece and the time the subject pressed a button. Accuracy was defined as the proportion correct responses regardless of the preceding cue. We conducted a 2 (expectancy) × 2 (stimulus) within-subjects MANOVA in SPSS on response times and the proportion correct responses. We used an alpha of 0.05 to determine significance of each factor on both measures of performance.

Initial inspection of individual datasets revealed that four of the subjects did not perform the task according to the instructions, responding by pressing the button according to the cue (hear “sweet” and press button for sweet or hear “tasteless” and press button for tasteless) rather than according to what oral stimulus they received, as evidenced by a 1% accuracy on the unexpected trials and perfect accuracy on expected trials (100%) and uncharacteristically fast response times (of 764 ± 182 ms relative to oral stimulus onset). Consequently, we did not include these datasets in further behavioral or neuroimaging analyses (leaving 16 datasets). The average accuracy for the remaining 16 subjects was 93 ± 8% (across both expected and unexpected trials) and their average reaction time was 2799 ± 1601 ms, which is consistent with published reports of taste detection response times (Bonnet et al., 1999; Veldhuizen et al., 2010). Analyses of the reaction times revealed a main effect of expectancy on response times ($F(1,15) = 25.710$, $p < 0.001$), with subjects responding faster to validly cued stimuli (Figure 3 upper panel). No main effect of stimulus was observed ($F(1,15) = 0.006$, $p = .942$), nor an interaction between expectancy and stimulus ($F(1,15) = .680$, $p = .422$).

A main effect of expectancy was also observed on accuracy, with subjects significantly more accurate in correctly detecting the stimulus following a valid cue ($F(1,15) = 10.625$, $p = .005$) (Figure 3 lower panel). We observed a trend for an effect of stimulus ($F(1,15) = 3.717$, $p = .073$); subjects are slightly more accurate in detecting the presence of a taste in the solution than they are at identifying the absence of a taste in the tasteless solution. We did not observe a significant interaction effect of expectancy and stimulus on accuracy ($F(1,15) = 1.734$, $p = .208$).

fMRI Data

Main effect of expectation: Regions responding preferentially when expectation is met—To determine which regions respond preferentially to expected vs. unexpected stimuli we compared the average response to the expected stimuli with the averaged response to the unexpected stimuli [ExpSwt + ExpTless] − [UnSwt + UnTless]. This yielded bilateral whole brain corrected responses in the fusiform gyrus, reflecting greater deactivation to receipt of unexpected compared to expected oral stimuli (Figure 4 and Table 1).

Main effect of expectation: Regions responding preferentially when expectation is breached—To determine which regions responded preferentially to the unexpected vs. the expected stimuli we compared the average response to the unexpected stimuli with the averaged response to the expected stimuli [UnSwt + UnTless] − [ExpSwt + ExpTless]. This resulted in widespread activation in gustatory, reward and attention networks. More specifically, significant effects were observed in the gustatory sensory pathway (ventroposteromedial thalamus, anterior insula) (Pritchard et al., 1986; Small, 2006), limbic regions important in the generation of error signals (anterior OFC and VS) (Tremblay and Schultz, 1999; Schultz et al., 2000; Tremblay and Schultz, 2000; O'Doherty et al., 2003), and in the attention network (inferior frontal gyrus, anterior cingulate cortex, IPS, and far anterior dorsal insula) (Nobre et al., 1999; Kanwisher and Wojciulik, 2000; Nobre, 2001; Corbetta and Shulman, 2002; Mesulam et al., 2005; Craig, 2009; Small, 2010) (Figure 5 and Table 2).

Interactions between expectation and stimulus—To isolate responses where breaches of expectation occurred preferentially for the sweet taste compared to the control stimulus we performed the double subtraction [UnSwt − ExpSwt] − [UnTless − ExpTless]). This resulted in a significant peak in a region of right dorsal anterior insula corresponding to human primary taste cortex as well as a weaker non-significant activation in the same area of the left hemisphere (Small, 2010) (Figure 6 and Table 3). No significant effects were observed for the opposite direction (greater effects of expectation on tasteless vs. taste). We also examined effects of expectation separately for the two stimuli (sweet and tasteless). UnSwt − ExpSwt produced significant activation in the insula, cingulate cortex, intrapariatal sulcus, and inferior frontal gyrus. Ventral striatal activation was observed when the threshold was lowered to $p < 0.005$, uncorrected (Table 4). UnTless − ExpTless produced significant responses in the insular cortex; however, activation in the cingulate, inferior frontal gyrus, and VS emerged at a lower threshold, $p < 0.005$, uncorrected (Table 5).

Connectivity—We observed greater responses to unexpected vs. expected oral stimulation in sensory, reward and attention regions. We hypothesized that the attention and reward networks might modulate incoming sensory signals to maximize information processing, with top-down modulation of incoming sensory signals from the attention system serving goal directed behavior (discrimination task) and modulation of incoming sensory signals by the reward system enhance information processing of biologically relevant sensations. To test this prediction we performed PPI analyses with the peaks from inferior frontal gyrus, anterior cingulate cortex, IPS, anterior OFC and VS. We observed greater connectivity between right IPS and left anterior insula ([−33 12 9], $Z = 3.81$, $P_{FDR} = .015$), between left VS and left anterior insula ([−33 21 3], $Z=3.31$, $P_{FDR} = .023$), and between right VS and bilateral anterior insula ([−33 21 3], $Z = 3.75$, $P_{FDR} = .016$, [36 21 −6], $Z = 3.40$, $P_{FDR} = .016$) under unexpected compared to expected oral stimulation (Figure 7). We also performed PPI analyses with peaks from anterior insula. Expectation did not influence connectivity between this region and VS or IPS.

The PPI analysis confirmed that expectation modulates connectivity between the IPS, VS and anterior insula. Next, to determine the direction of the influences and interactions between these regions we used DCM to test all possible models of information flow through this network. Based on the (across hemisphere) regions identified in the PPI analysis we specified an across-hemisphere network of the following regions: right IPS, right VS, and left anterior insula. Taste and tasteless events (collapsed across expectancy) were used as driving inputs entered all models through the anterior insula (Figure 8A). All models were specified to have bidirectional "steady state" connectivity (intrinsic connections) between all three areas, except between the VS and parietal cortex as connections from the striatum to the cortex must pass through the pallidum and thalamus, which were not included in the model (Figure 8A). Responses from unexpected and expected events (collapsed across stimulus) were used as modulatory inputs on each of the intrinsic connections to create all possible models (31). The five connections that we varied the modulatory influences for were: 1) the connection from IPS to VS, 2) from IPS to anterior insula, 3) from VS to anterior insula, 4) from anterior insula to IPS, and 5) from anterior insula to VS. We used fixed effects Bayesian model selection to compare all models using the free energy approximation to the log-evidence for each model (Stephan et al., 2009). The free energy formulation contains terms for both model accuracy and complexity (Stephan et al., 2009). Thus more complex models are not necessary better. The log model evidence is also used to compute the conditional probability for each model across all 31 models. A fixed effects analysis assumes that all subjects are using the same model architecture. This assumption is considered to be appropriate when the subjects are relatively homogenous (ours were all young women) and the processes being studied are basic physiologic or attentional mechanisms that are unlikely to vary across the subject group (Penny et al., 2010; Stephan et al., 2010; Desseilles et al., 2011). Bayesian model selection demonstrated that there was significant evidence (posterior probability = 0.954) in favor of model 19 (modulation of parietal to insula, VS to insula and insula to VS) (Figure 8B and C). Thus these results support our hypothesis that both parietal cortex and VS influence response in the anterior insula, reflecting modulation of sensory inputs by attentional and reward networks, respectively. However, they also indicate that insular responses modulate VS, which may reflect the interaction between sensory and reward processing.

Discussion

Our experiment yielded four novel findings. First, unexpected oral stimulation resulted in robust recruitment of attention, gustatory, and reward networks. This is in keeping with the need to orient towards, identify, and learn about biologically relevant unexpected oral stimulation. Second, that the influence of a breach of expectation was greater in the anterior dorsal insula when the unexpected oral stimulus contained a taste. This suggests that while unexpected oral stimulation results in enhanced recruitment of taste, reward and attentional networks, gustatory signals are integrated with attention and/or reward signals specifically in the anterior dorsal insula. Third, that the VS and IPS preferentially interact with insular cortex during unexpected vs. expected tasting, with DCM indicating that connectivity from the parietal cortex and VS to the anterior insula and from the anterior insula to VS is enhanced by unexpected tastes. Finally, we report one unpredicted finding; receipt of an unexpected vs. an expected oral stimulus was associated with greater suppression in the fusiform gyri, which forms part of the visual object recognition stream (Haxby et al., 1991). We suggest that this result may reflect cross-modal suppression during a taste object identification task.

Breaches of taste expectation recruit attention gustatory and reward circuits

It has long been known that the sensation of an unexpected event during goal-directed behavior is associated with attentional deployment and re-orientation (Posner, 1980). Consistent with findings from classical studies of visual spatial attention (Posner, 1980) we found that reaction times were significantly slower, and detection less accurate, following invalid compared to valid cueing (Figure 3). We therefore suggest our results reflect the behavioral cost of attentional deployment and stimulus identity reorientation following the breach of taste expectation. As such, breaches of taste identity expectation resulted in preferential recruitment of regions critical for attentional control including the IPS, inferior frontal gyrus, and anterior cingulate cortex (Mesulam et al., 2005). Moreover, the IPS and inferior frontal gyrus have been specifically implicated in reorienting to location following invalid cues in both visual and tactile domains (Corbetta and Shulman, 2002; Macaluso et al., 2002) and in reorienting to time following invalid cues (Corbetta et al., 1998; Nobre, 2001). Thus our finding aligns with work highlighting the supra-modal nature of the fronto-parietal attention network.

We also observed preferential responses in the anterior OFC and VS during breaches of taste identity expectation. Both regions have been implicated by functional neuroimaging studies in coding error signals in the context of reward learning (Pagnoni et al., 2002; McClure et al., 2003; O'Doherty et al., 2003), with the magnitude of responses modulated according to the strength of an error signal thought to be generated (O'Doherty et al., 2003). The anterior OFC has also been shown to respond to taste (Small et al., 2003; Verhagen and Engelen, 2006), and breaches of visual spatial expectation (Nobre et al., 1999). In our task invalid trials were associated not only with attentional reorientation, but also the generation of a positive or a negative error signal; negative if sweet was expected and tasteless received, or positive if tasteless was expected and sweet received. Therefore the preferential response in the OFC could reflect sensory, reward or attentional processing; or perhaps an integration of the three processes (Maunsell, 2004).

Likewise, preferential recruitment of the anterior insular cortex during breaches of taste identity expectation may reflect attentional, reward or sensory processing. This region corresponds to primary taste cortex (Pritchard et al., 1986) and consistently responds to taste stimuli (Frey and Petrides, 1999; Zald and Pardo, 2000; O'Doherty et al., 2001). However, it is also sensitive to expectation and attention. The insula is activated during general selective attention (Nobre, 2001; Corbetta and Shulman, 2002), "oddball" tasks, which require reorientation, (Linden et al., 1999; Huettel and McCarthy, 2004), and risk prediction and risk assessment (Preuschoff et al., 2008). It is also thought to play a critical role in attending to interoceptive stimuli (Critchley et al., 2004) and in self awareness (Craig, 2009). To integrate the seemingly disparate insular functions, Menon and Uddin have argued that the insular cortex plays a general role in the attribution of salience to environmental events in order to mark them in time and place for additional processing (Menon and Uddin, 2010). It is therefore possible that the enhanced insular responses to unexpected tastes reflects orienting to the mouth following a breach of expectation, assessment of the risk of consuming the substance or general salience attribution to the unexpected taste.

Evidence that gustatory signals are integrated with attention and/or reward signals in the anterior dorsal insula

Selective attention to taste alters taste-evoked responses in rodents and humans (Fontanini and Katz, 2005; Veldhuizen et al., 2007; Fontanini and Katz, 2009). In primates, neurons in the primary taste cortex not only respond to the sensation of a taste but also to the sight of an approaching syringe that delivers the taste (Scott and Plata-Salaman, 1999). In humans, leading subjects to expect delivery of the weaker compared to the stronger bitter stimulus

results in reduced insular response to the stronger stimulus, indicating that expectations about intensity can change taste perception and that this modulation depends upon processes in insular cortex (Nitschke et al., 2006). In keeping with these findings we found greater response in the insula to a breach of expectation when the oral stimulus contained a taste. This indicates that within this region of insular cortex, sensory signals interact with attentional and reward signals, possibly in the service of assigning greater saliency to the taste sensation (O'Doherty et al., 2003; Menon and Udin, 2010). One caveat to this interpretation is that we cannot rule out the possibility that it is the positive error signal rather than the taste that recruits the insula. However we feel this is unlikely since the region corresponds to primary taste cortex (Small, 2010) and prior studies of error signaling using gustatory stimuli have failed to find responses in insular cortex related to error signal generation (either positive or negative) (Berns et al., 2001; Pagnoni et al., 2002; McClure et al., 2003; O'Doherty et al., 2003; O'Doherty et al., 2006).

Evidence for greater connectivity between insula, striatum and IPS during breaches of expectation

Breaches of taste expectation recruited multiple regions. To test whether these co-activations reflected greater inter-connectivity we extracted responses from the most significantly activated voxels within the IPS and VS and asked if the interaction between these seed regions and all other brain areas depended upon expectation. Both the IPS and the VS exhibited preferential connectivity specifically with the anterior insula during unexpected vs. expected tasting (Figure 7). This indicates that these critical nodes of the attention, reward and gustatory networks are not simply co-activated, but also preferentially interact during breaches of oral sensory expectation. We predicted that IPS and VS would influence insular responses, reflecting upregulation of sensory processing by reward and attention networks. Thirty-one DCM models were generated with inputs entering at the anterior insula to reflect the gustatory task. There was significant evidence for one model that showed modulation of IPS on insula, VS on insula, and insula on VS. Thus these results support our hypothesis that both parietal cortex and VS influence response in the anterior insula, reflecting modulation of sensory inputs by attentional and reward networks, respectively. They also indicate that the connection between the VS and insula represents bi-directional influences.

Evidence for cross-modal interactions

Finally, an unanticipated finding was that unexpected compared to expected tasting was associated with significantly greater de-activations in the fusiform gyrus bilaterally. The fusiform gyrus is part of the ventral stream for visual object recognition (Haxby et al., 1991). Prior studies of cross-modal interactions show that attending to one modality may result in decreased responses in the other (Mozolic et al., 2008). Our task required subjects to identify taste stimuli. We therefore suggest that the effect observed in fusiform gyrus reflects cross-modal suppression of visual object identification during this taste identification task. We further speculate that the deactivation was greater when the stimulus is unexpected because greater attentional resources were necessary to taste and identify the unexpected stimulus, making those resources less available to other modalities. An alternative possibility is that the de-activation reflects active suppression of conflicting sensory input (Laurienti et al., 2002). However, we suggest that this is unlikely, because our subjects were instructed to keep their eyes closed during scanning.

In summary, we demonstrated that unexpected oral stimulation results in up-regulation of taste sensory cortex by attention and reward networks and down regulation of the region of visual cortex important for object recognition. These findings are consistent with the need for coordinated activity of multiple networks to help organisms orient towards, identify and learn about biologically relevant. One caveat is that all of our subjects were women. It is not

possible to know if the observed effects will generalize to men. Future work is needed to evaluate the importance of phenotypes such as gender, body weight and eating style on these responses.

Acknowledgments

This study was supported by grant AS 299/1-1 (research fellowship) from the German Research Foundation (Deutsche Forschungsgemeinschaft: DFG) to KA and by NIDCD R016706-01 awarded to DMS.

Abbreviations

VS	ventral striatum
IPS	intraparietal sulcus
OFC	orbitofrontal cortex
AI	anterior insula

References

Accolla R, Bathellier B, Petersen CCH, Carleton A. Differential Spatial Representation of Taste Modalities in the Rat Gustatory Cortex. J Neurosci. 2007; 27:1396–1404. [PubMed: 17287514]

Bartoshuk LM, McBurney DH, Pfaffmann C. Taste of Sodium Chloride Solutions after Adaptation to Sodium Chloride: Implications for the “Water Taste”. Science. 1964; 143:967–968. [PubMed: 14090150]

Bartoshuk LM, Duffy VB, Hayes JE, Moskowitz HR, Snyder DJ. Psychophysics of sweet and fat perception in obesity: problems, solutions and new perspectives. Philos T Roy Soc B. 2006; 361:1137–1148.

Bender G, Veldhuizen MG, Meltzer JA, Gitelman DR, Small DM. Neural correlates of evaluative compared with passive tasting. Eur J Neurosci. 2009; 30:327–338. [PubMed: 19614981]

Berns GS, McClure SM, Pagnoni G, Montague PR. Predictability modulates human brain response to reward. J Neurosci. 2001; 21:2793–2798. [PubMed: 11306631]

Bonnet C, Zamora MC, Buratti F, Guirao M. Group and individual gustatory reaction times and Pieron’s law. Physiol Behav. 1999; 66:549–558. [PubMed: 10386896]

Corbetta M, Shulman GL. Control of goal-directed and stimulus-driven attention in the brain. Nat Rev Neurosci. 2002; 3:201–215. [PubMed: 11994752]

Corbetta M, Akbudak E, Conturo TE, Snyder AZ, Ollinger JM, Drury HA, Linenweber MR, Petersen SE, Raichle ME, Van Essen DC, Shulman GL. A common network of functional areas for attention and eye movements. Neuron. 1998; 21:761–773. [PubMed: 9808463]

Craig AD. How do you feel - now? The anterior insula and human awareness. Nat Rev Neurosci. 2009; 10:59–70. [PubMed: 19096369]

Critchley HD, Wiens S, Rotshtein P, Ohman A, Dolan RJ. Neural systems supporting interoceptive awareness. Nat Neurosci. 2004; 7:189–195. [PubMed: 14730305]

Desseilles M, Schwartz S, Dang-Vu TT, Sterpenich V, Ansseau M, Maquet P, Phillips C. Depression alters “top-down” visual attention: A dynamic causal modeling comparison between depressed and healthy subjects. NeuroImage. 2011; 54:1662–1668. [PubMed: 20807578]

Felsted JA, Ren X, Chouinard-Decorte F, Small DM. Genetically Determined Differences in Brain Response to a Primary Food Reward. J Neurosci. 2010; 30:2428–2432. [PubMed: 20164326]

Fontanini A, Katz DB. 7 to 12 Hz activity in rat gustatory cortex reflects disengagement from a fluid self-administration task. J Neurophys. 2005; 93:2832–2840.

Fontanini A, Katz DB. Behavioral modulation of gustatory cortical activity. Ann N Y Acad Sci. 2009; 1170:403–406. [PubMed: 19686167]

Frey S, Petrides M. Re-examination of the human taste region: a positron emission tomography study. Eur J Neurosci. 1999; 11:2985–2988. [PubMed: 10457193]

Friston KJ, Harrison L, Penny W. Dynamic causal modelling. Neuroimage. 2003; 19:1273–1302. [PubMed: 12948688]

Friston KJ, Buechel C, Fink GR, Morris J, Rolls E, Dolan RJ. Psychophysiological and modulatory interactions in neuroimaging. Neuroimage. 1997; 6:218–229. [PubMed: 9344826]

Gitelman DR, Penny WD, Ashburner J, Friston KJ. Modeling regional and psychophysiologic interactions in fMRI: the importance of hemodynamic deconvolution. NeuroImage. 2003; 19:200–207. [PubMed: 12781739]

Green BG, Dalton P, Cowart B, Shaffer G, Rankin K, Higgins J. Evaluating the 'labeled magnitude scale' for measuring sensations of taste and smell. Chem Sens. 1996; 21:323–334.

Haxby JV, Grady CL, Horwitz B, Ungerleider LG, Mishkin M, Carson RE, Herscovitch P, Schapiro MB, Rapoport SI. Dissociation of object and spatial visual processing pathways in human extrastriate cortex. Proc Natl Acad Sci U S A. 1991; 88:1621–1625. [PubMed: 2000370]

Henson RN, Price CJ, Rugg MD, Turner R, Friston KJ. Detecting latency differences in event-related BOLD responses: application to words versus nonwords and initial versus repeated face presentations. Neuroimage. 2002; 15:83–97. [PubMed: 11771976]

Huettel SA, McCarthy G. What is odd in the oddball task?: Prefrontal cortex is activated by dynamic changes in response strategy. Neuropsychologia. 2004; 42:379–386. [PubMed: 14670576]

Kanwisher N, Wojciulik E. Visual attention: insights from brain imaging. Nat Rev Neurosci. 2000; 1:91–100. [PubMed: 11252779]

Katz DB, Nicolelis MA, Simon SA. Gustatory processing is dynamic and distributed. Curr Opin Neurobiol. 2002; 12:448–454. [PubMed: 12139994]

Laurienti PJ, Burdette JH, Wallace MT, Yen YF, Field AS, Stein BE. Deactivation of sensory-specific cortex by cross-modal stimuli. J Cogn Neurosci. 2002; 14:420–429. [PubMed: 11970801]

Linden DEJ, Prvulovic D, Formisano E, VÃöllinger M, Zanella FE, Goebel R, Dierks T. The Functional Neuroanatomy of Target Detection: An fMRI Study of Visual and Auditory Oddball Tasks. Cereb Cortex. 1999; 9:815–823. [PubMed: 10601000]

Macaluso E, Frith CD, Driver J. Supramodal effects of covert spatial orienting triggered by visual or tactile events. J Cogn Neurosci. 2002; 14:389–401. [PubMed: 11970799]

Macey PM, Macey KE, Kumar R, Harper RM. A method for removal of global effects from fMRI time series. NeuroImage. 2004; 22:360–366. [PubMed: 15110027]

Maunsell JHR. Neuronal representations of cognitive state: reward or attention? Trends Cog Sci. 2004; 8:261–265.

McClure SM, Berns GS, Montague PR. Temporal prediction errors in a passive learning task activate human striatum. Neuron. 2003; 38:339–346. [PubMed: 12718866]

McClure SM, Li J, Tomlin D, Cypert KS, Montague LM, Montague PR. Neural correlates of behavioral preference for culturally familiar drinks. Neuron. 2004; 44:379–387. [PubMed: 15473974]

Menon V, Uddin L. Saliency, switching, attention and control: a network model of insula function. Brain Struct Funct. 2010; 214:655–667. [PubMed: 20512370]

Mesulam, M.; Small, DM.; Vandenberghe, R.; Gitelman, DR.; Nobre, AC. A heteromodal large-scale network for spatial attention. In: Itti, L.; Rees, G.; Tsotsos, J., editors. Neurobiology of Attention. San Diego, CA: Elsevier Academic Press; 2005. p. 29-34.

Mozolic J, Joyner D, Hugenschmidt C, Peiffer A, Kraft R, Maldjian J, Laurienti P. Cross-modal deactivations during modality-specific selective attention. BMC Neurology. 2008; 8:35. [PubMed: 18817554]

Nitschke JB, Dixon GE, Sarinopoulos I, Short SJ, Cohen JD, Smith EE, Kosslyn SM, Rose RM, Davidson RJ. Altering expectancy dampens neural response to aversive taste in primary taste cortex. Nat Neurosci. 2006; 9:435–442. [PubMed: 16462735]

Nobre AC. Orienting attention to instants in time. Neuropsychologia. 2001:39.

Nobre AC, Coull JT, Frith CD, Mesulam MM. Orbitofrontal cortex is activated during breaches of expectation in tasks of visual attention. Nat Neurosci. 1999; 2:11–12. [PubMed: 10195173]

O'Doherty J, Rolls ET, Francis S, Bowtell R, McGlone F. Representation of pleasant and aversive taste in the human brain. J Neurophys. 2001; 85:1315–1321.

O'Doherty JP, Buchanan TW, Seymour B, Dolan RJ. Predictive neural coding of reward preference involves dissociable responses in human ventral midbrain and ventral striatum. Neuron. 2006; 49:157–166. [PubMed: 16387647]

O'Doherty JP, Dayan P, Friston K, Critchley H, Dolan RJ. Temporal difference models and reward-related learning in the human brain. Neuron. 2003; 38:329–337. [PubMed: 12718865]

Oldfield RC. The assessment and analysis of handedness: the Edinburgh inventory. Neuropsychologia. 1971; 9:97–113. [PubMed: 5146491]

Pagnoni G, Zink CF, Montague PR, Berns GS. Activity in human ventral striatum locked to errors of reward prediction. Nat Neurosci. 2002; 5:97–98. [PubMed: 11802175]

Penny WD, Stephan KE, Daunizeau J, Rosa MJ, Friston KJ, Schofield TM, Leff AP. Comparing Families of Dynamic Causal Models. PLoS Comput Biol. 2010; 6:e1000709. [PubMed: 20300649]

Plassmann H, O'Doherty J, Shiv B, Rangel A. Marketing actions can modulate neural representations of experienced pleasantness. Proc Natl Acad Sci U S A. 2008; 105:1050–1054. [PubMed: 18195362]

Posner MI. Orienting of attention. Q J Exp Psychol. 1980; 32:3–25. [PubMed: 7367577]

Preuschoff K, Quartz SR, Bossaerts P. Human Insula Activation Reflects Risk Prediction Errors As Well As Risk. The Journal of Neuroscience. 2008; 28:2745–2752. [PubMed: 18337404]

Pritchard TC, Hamilton RB, Morse JR, Norgren R. Projections of thalamic gustatory and lingual areas in the monkey, Macaca fascicularis. J Comp Neurol. 1986; 244:213–228. [PubMed: 3950095]

Rescorla, RA.; Wagner, AR. A theory of Pavlovian conditioning: Variations in the effectiveness of reinforcement and nonreinforcement. In: Black, AH.; Prokasy, WF., editors. Classical conditioning II. New York: Appleton-Century-Crofts; 1972.

Schultz W, Tremblay L, Hollerman JR. Reward Processing in Primate Orbitofrontal Cortex and Basal Ganglia. Cereb Cortex. 2000; 10:272–283. [PubMed: 10731222]

Scott TR, Plata-Salaman CR. Taste in the monkey cortex. Physiol Behav. 1999; 67:489–511. [PubMed: 10549886]

Small D. Taste representation in the human insula. Brain Struct Funct. 2010; 214:551–561. [PubMed: 20512366]

Small, DM. Central Gustatory Processing in Humans. In: Hummel, T.; Welge-Lüssen, A., editors. Taste and Smell An Update Adv Otorhinolaryngol. Basel: Karger; 2006. p. 191-220.

Small DM, Veldhuizen MG, Felsted J, Mak YE, McGlone F. Separable Substrates for Anticipatory and Consummatory Food Chemosensation. Neuron. 2008; 57:786–797. [PubMed: 18341997]

Small DM, Gregory MD, Mak YE, Gitelman D, Mesulam MM, Parrish T. Dissociation of Neural Representation of Intensity and Affective Valuation in Human Gustation. Neuron. 2003; 39:701–711. [PubMed: 12925283]

Small DM, Voss J, Mak YE, Simmons KB, Parrish T, Gitelman D. Experience-dependent neural integration of taste and smell in the human brain. J Neurophys. 2004; 92:1892–1903.

Stephan KE, Penny WD, Daunizeau J, Moran RJ, Friston KJ. Bayesian model selection for group studies. NeuroImage. 2009; 46:1004–1017. [PubMed: 19306932]

Stephan KE, Penny WD, Moran RJ, den Ouden HEM, Daunizeau J, Friston KJ. Ten simple rules for dynamic causal modeling. NeuroImage. 2010; 49:3099–3109. [PubMed: 19914382]

Talairach, J.; Tournoux, P. Co-planar stereotaxic atlas of the human brain. New York: Thieme; 1998.

Tremblay L, Schultz W. Relative reward preference in primate orbitofrontal cortex. Nature. 1999; 398:704–708. [PubMed: 10227292]

Tremblay L, Schultz W. Modifications of reward expectation-related neuronal activity during learning in primate orbitofrontal cortex. J Neurophys. 2000; 83:1877–1885.

Veldhuizen MG, Small DM. Modality-Specific Neural Effects of Selective Attention to Taste and Odor. Chem Sens. 2011

Veldhuizen MG, Bender G, Constable RT, Small DM. Trying to Detect Taste in a Tasteless Solution: Modulation of Early Gustatory Cortex by Attention to Taste. Chem Sens. 2007; 32:569–581.

Veldhuizen MG, Shepard TG, Wang M-F, Marks LE. Coactivation of Gustatory and Olfactory Signals in Flavor Perception. Chem Sens. 2010; 35:121–133.

Verhagen JV, Engelen L. The neurocognitive bases of human multimodal food perception: sensory integration. Neurosci Biobehav Rev. 2006; 30:613–650. [PubMed: 16457886]

Wagner, AR.; Rescorla, RA. Inhibition in Pavlovian conditioning: Application of a theory. In: Boakes, RA.; Halliday, MS., editors. Inhibition and Learning. London: Academic Press; 1972.

Zald DH, Pardo JV. Cortical activation induced by intraoral stimulation with water in humans. Chem Sens. 2000; 25:267–275.

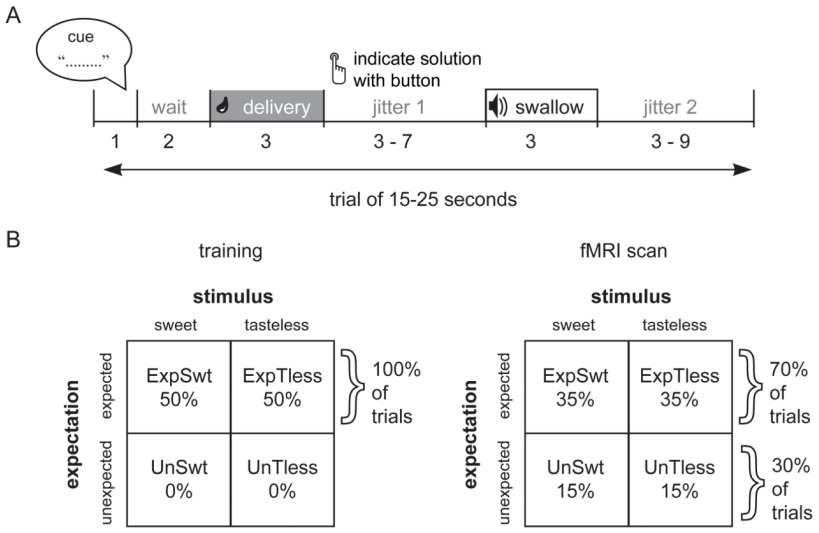

Figure 1. Experimental design

A. Timeline of events within a trial. Events lasted 15 – 25 seconds with an average length of 20 seconds. Each event began with a 1-second vocal cue announcing either "sweet" or "tasteless", a 2 second wait period, after which sucrose or tasteless solution was presented (0.5 ml over 3 seconds). Subjects were asked to indicate which solution they received by pressing a button on a button box as fast as they could during jitter 1 (various lengths that were randomized over trials). Then a 1-second swallow tone indicated that the subjects were allowed to swallow the liquid. After jitter 2 (various lengths that were randomized over trials) a new trial began.

B. Graphical depiction of design. During training (left) all trials were valid (ExpSwt = validly cued sweet delivery and ExpTless − validly cued tasteless delivery). During the fMRI scanning only 70% of the events were valid. The remaining 30% were invalid trials in which subjects heard "tasteless" but received sweet (UnSwt) or heard "sweet" and received tasteless (UnTless).

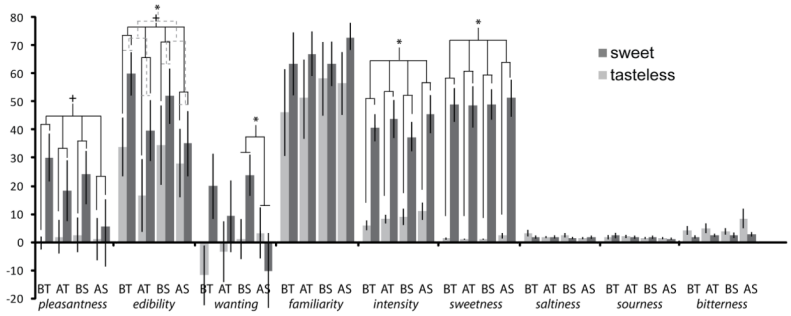

Figure 2. Intensity and pleasantness ratings of the four different events of interest

We plotted mean pleasantness, edibility, wanting and familiarity (rated on VAS-scales) and intensity, sweetness, saltiness, sourness and bitterness (rated on a gLMS-scale) ratings (averaged over subjects, +/− standard error of the mean), against time and session (x-axis). The abbreviations indicating time and session are: BT, before training, AT, after training, BS, before scan, and AS, after scan. Dark grey bars stand for the sweet stimuli and light grey bars for the tasteless stimuli. Sweet stimuli are perceived to be significantly more intense and sweet (indicated by * ($p<.05$)), a trend for sweet to be rated as more edible and pleasant (indicated by + ($p<0.1$)). Edibility ratings were lower before the sessions than after the sessions (indicated by * ($p<.05$)). There was a significant decrease in wanting of either stimulus before compared to after the scanning session (indicated by * ($p<.05$)).

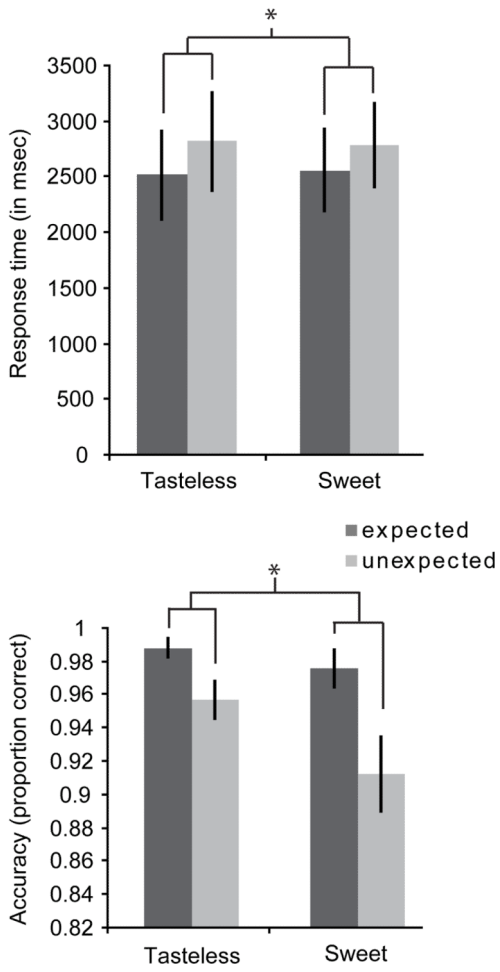

Figure 3. Response times and proportion correct responses of the four different events of interest

In the top and bottom panels we plotted response times (in ms) and proportion correct responses respectively (averaged over subjects, +/− standard error of the mean), against stimulus (x-axis). Dark grey bars stand for the expected events and light grey bars for the unexpected events. Expected events were responded to faster and more accurately (indicated by * ($p<.05$)).

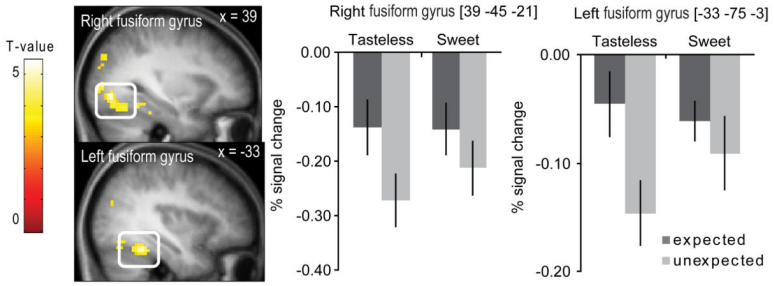

Figure 4. Neural response to expected vs. unexpected events

Sagittal sections show neural response to expected vs. unexpected oral stimuli [ExpSwt + ExpTless] − [UnSwt + UnTless] in bilateral fusiform gyrus. The bar graphs show on the y-axis the percent signal change for the expected (in dark grey) and unexpected (light grey) events (+/− standard error of the mean.), averaged over subjects. On the x-axis are the stimuli. The response was taken from the voxel that responded maximally within the significant cluster, as identified in the SPM analysis. Color bar depicts T-values.

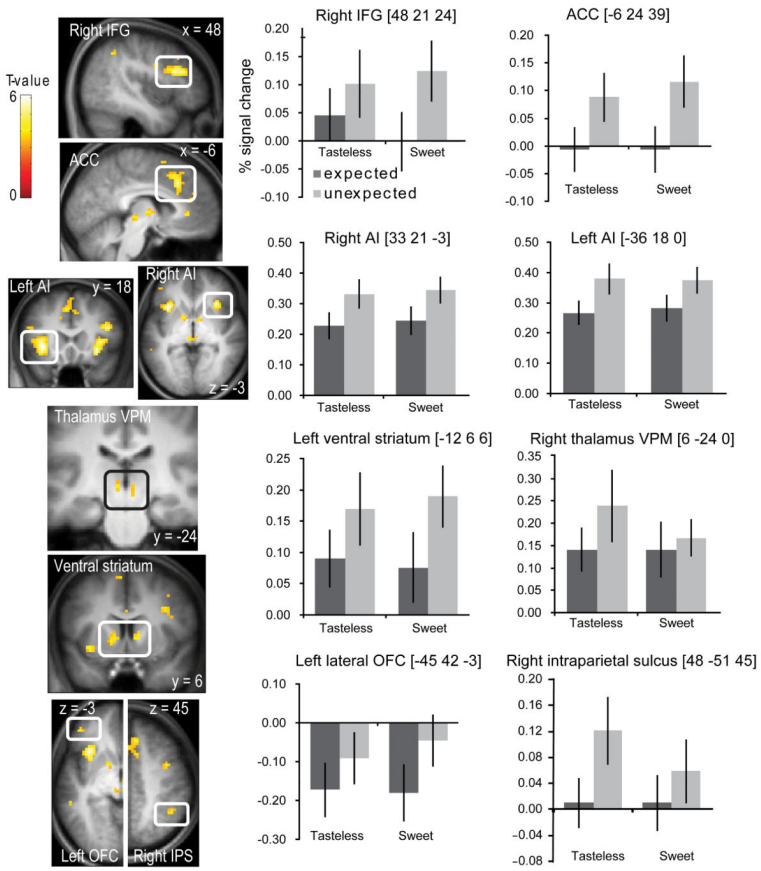

Figure 5. Neural response to unexpected vs. expected events

Sections show neural response to unexpected vs. expected oral stimuli [UnSwt + UnTless] − [ExpSwt + ExpTless] in right inferior frontal gyrus (IFG), anterior cingulate cortex (ACC), bilateral anterior insula (AI), bilateral ventroposteromedial (VPM) thalamus, and bilateral VS. The bar graphs show on the y-axis the percent signal change for the expected (in dark grey) and unexpected (light grey) events (+/− standard error of the mean), averaged over subjects. On the x-axis are the stimuli. The response was taken from the voxel that responded maximally within the significant cluster, as identified in the SPM analysis. Color bar depicts T-values.

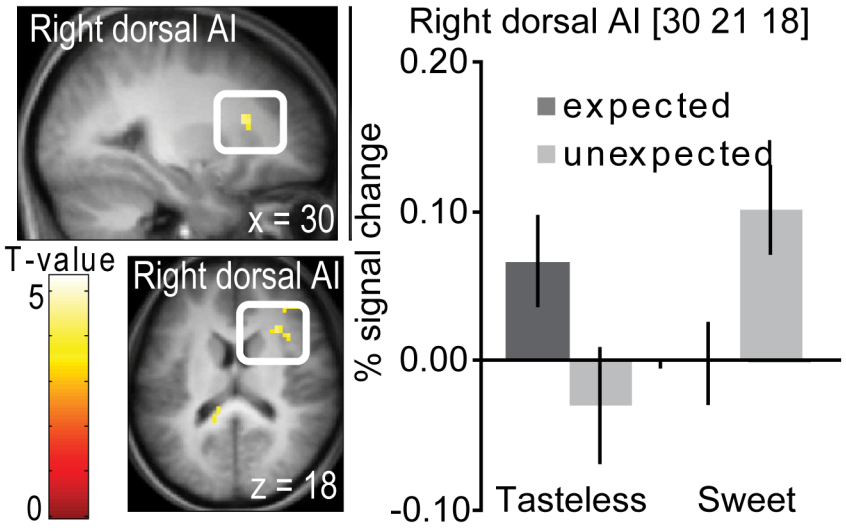

Figure 6. Neural response to unexpectedly receiving a sweet stimulus compared to unexpectedly receiving a tasteless solution

Sagittal section shows neural response in right dorsal AI to unexpectedly receiving a sweet stimulus specifically ([UnSwt − ExpSwt] − [UnTless − ExpTless]). The bar graphs show on the y-axis the percent signal change for the expected (in dark grey) and unexpected (light grey) events (+/− standard error of the mean), averaged over subjects. On the x-axis are the stimuli. The response was taken from the voxel that responded maximally within the significant cluster, as identified in the SPM analysis. Color bar depicts T-values.

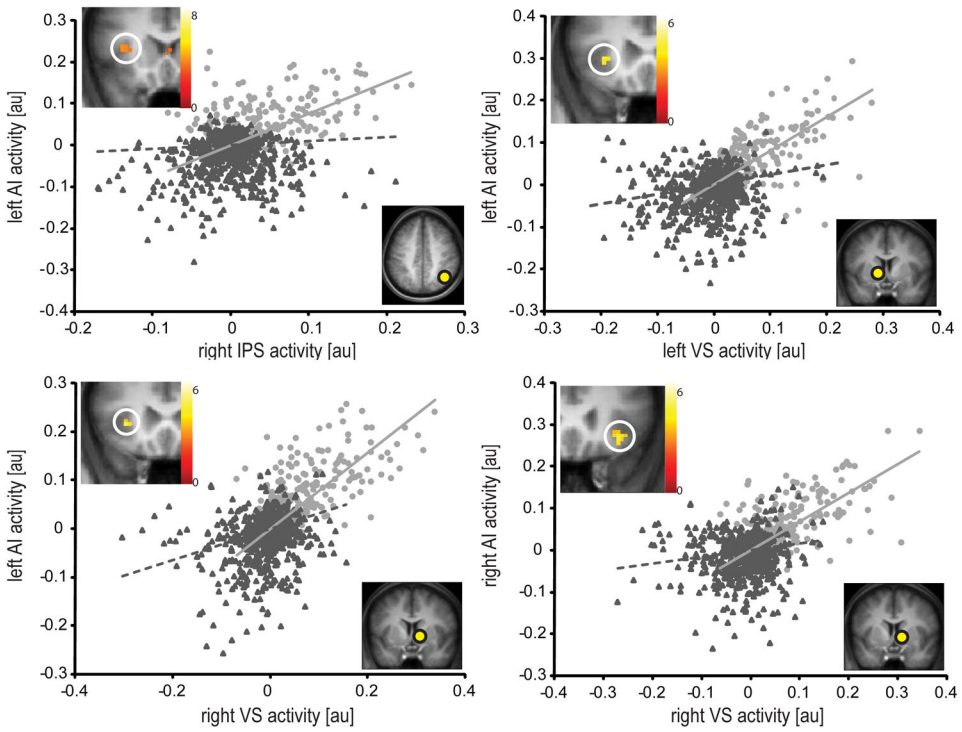

Figure 7. Psychophysiological interaction results

Regression of activity in anterior insula (AI) on the activity in the seed regions IPS and VS when the oral stimulus was unexpected (light grey circles and solid grey line) versus expected (dark grey triangles and dotted dark line). Each observation corresponds to the time series interaction with that condition. The section by the x-axis show the location of the seed region, and the section next to the y-axis shows the neural response in anterior insula that was significantly associated with a stronger connectivity under unexpected vs. expected with the seed region. Color bar depicts T-values.

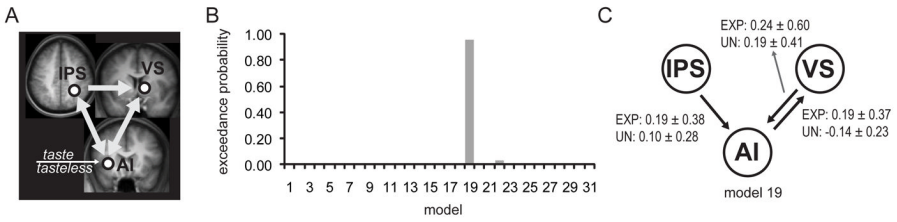

Figure 8. DCM models and model evidence

A. **Invariable configuration of all network models.** Taste and tasteless events (collapsed across expectancy) were used as driving inputs into the anterior insula (AI), and all models were specified to have full "steady state" connectivity between the nodes in the network.

B. **Exceedance probabilities of all 31 possible models.** The exceedance probability is the probability that a model is more likely than any of the other models given the observed fMRI data. Exceedance probabilities showed significant evidence in favor of model 19.

C. **Configuration of model 19.** For model 19 modulation of AI by VS and IPS, and modulation of VS by AI was specified. Average estimates (arbitrary units, ± sd) of modulation strength across subjects of each of the modulatory inputs (unexpected and expected events collapsed across stimulus) are depicted next to each of the intrinsic connections.

Table 1

Significant peaks of [ExpSwt + ExpTless] − [UnSwt + UnTless]

Area	*x, y, z* MNI[a]	K[b]	Z	P_{FDR}[c]
Left fusiform gyrus	−33 −75 −3	174	4.89	0.018
	−30 −84 6		4.41	0.027
	−45 −72 −3		4.08	0.069
Right fusiform gyrus	39 −45 −21	104	4.63	0.023
	48 −57 −15		4.18	0.049
	48 −54 −6		3.80	0.086

[a] Italics indicate that a peak falls under the same cluster as the preceding peak

[b] Cluster size in voxels

[c] Significant at $P_{FDRcorrected} = 0.05$ across the whole brain

Table 2

Significant peaks of [UnSwt + UnTless] − [ExpSwt + ExpTless]

Area	*x, y, z* MNI[a]	K[b]	Z	P_{FDR}[c]
Left anterior insula	−36 18 0	195	5.39	0.001
	−33 12 −6		4.75	0.002
	−33 30 6		3.87	0.013
Right anterior insula	33 21 −3	99	5.30	0.001
Right inferior frontal gyus	48 21 24	164	4.93	0.001
	48 30 24		4.79	0.002
	42 0 30		4.18	0.007
Anterior cingulate cortex	−6 24 39	334	4.81	0.001
	6 36 51		4.30	0.005
	9 36 9		4.29	0.005
Medial superior frontal gyrus	15 42 39	14	4.51	0.003
Left VS	−6 −9 6	70	4.08	0.008
	−12 3 3		3.99	0.010
	3 −12 3		3.55	0.025
Right middle frontal gyrus	42 3 45	9	3.94	0.012
Right VS	12 6 6	22	3.93	0.012
Right middle frontal gyrus	42 30 39	7	3.78	0.017
Left inferior frontal sulcus	−27 45 15	10	3.77	0.017
Right IPS	48 −51 45	6	3.73	0.019
Anterior cingulate cortex (at genu)	−6 36 3	7	3.73	0.019
Right middle temporal gyrus	57 −30 −9	21	3.71	0.019
	66 −33 −9		3.65	0.022
Left thalamus (ventroposteromedial)	−6 −24 0	30	3.71	0.019
Right thalamus	*3 −15 −6*		3.67	0.021
Right thalamus	*6 −24 0*		3.36	0.036
Posterior cingulate cortex	9 −66 39	8	3.70	0.020
Left lateral orbital gyrus	−45 42 −3	10	3.68	0.021
Anterior cingulate cortex	−6 6 63	5	3.42	0.032
Left inferior frontal gyrus	−48 18 21	11	3.42	0.032

[a] Italics indicate that a peak falls under the same cluster as the preceding peak

[b] Cluster size in voxels

[c] Significant at $P_{FDRcorrected} = 0.05$ across the whole brain

Table 3

Significant peaks of [UnSwt − ExpSwt] − [UnTless − ExpTless]

Area	*x, y, z* MNI[a]	K[b]	Z	P_{FDR}[c]
Right dorsal anterior insula	30 21 18	16	3.42	0.024
	39 18 18		3.42	0.026
Left dorsal anterior insula	−27 21 18	4	2.93	n.s.

[a] Italics indicate that a peak falls under the same cluster as the preceding peak

[b] Cluster size in voxels

[c] Significant at $P_{FDRcorrected} = 0.05$ across the ROIs

Table 4

Significant peaks of UnSwt − ExpSwt

Area	*x, y, z* MNI[a]	K[b]	Z	P_{FDR}
Right inferior frontal gyrus	48 30 24	123	4.94	0.022 [c]
	48 21 30		4.54	0.038 [c]
	39 18 18		3.95	0.044 [c]
Left anterior calcarine sulcus	−33 −69 9	7	4.25	0.042 [c]
Right IPS	51 −48 42	31	4.22	0.042 [c]
Left inferior frontal gyrus	−45 15 21	13	4.19	0.042 [c]
Anterior cingulate cortex	0 3 30	17	4.18	0.042 [c]
Anterior cingulate cortex	−9 21 36	61	4.17	0.042 [c]
Left ventral insula	−42 −9 −6	12	4.13	0.042 [c]
Left inferior frontal sulcus	−27 45 15	23	4.09	0.042 [c]
Anterior cingulate cortex	6 27 18	17	4.09	0.042 [c]
Anterior cingulate cortex	6 45 39	9	3.95	0.044 [c]
Right ventral insula	33 21 −6	17	3.77	0.010 [d]
	33 9 −9			0.002 [d]
Left anterior insula	−33 18 0	8	3.57	0.003 [d]
Left ventral insula	−33 9 −6	7	3.56	0.006 [d]
Right anterior insula	33 27 3	13	3.54	0.003 [d]
	36 18 6		3.24	0.003 [d]
Left ventral insula	−42 −9 −6	26	4.13	0.042 [c]
Left inferior frontal sulcus	−27 45 15	47	4.09	0.042 [c]
	6 27 18	47	4.09	0.042 [c]
Anterior cingulate cortex	48 −27 −9	32	3.79	n.s.
	54 −33 −6		2.97	n.s.
Superior colliculus	0 −39 −9	14	3.60	n.s.
Mediodorsal thalamus	0 −12 3	32	3.44	n.s.
	−15 −12 9		3.02	n.s.
	0 −21 3		2.94	n.s.
Left anterior orbital gyrus	−33 48 −9	6	3.40	n.s.
Left anterior orbital gyrus	−21 57 −3	5	3.40	n.s.
Right ventral/dorsal striatum	12 9 9	18	3.36	n.s.
	18 0 6		2.91	n.s.
	12 3 15		2.72	n.s.
Posterior cingulate sulcus	9 −66 39	16	3.34	n.s.
	9 −78 36		3.04	n.s.
Medial geniculate body	−9 −27 −12	6	3.28	n.s.

Area	*x, y, z* MNI[a]	K[b]	Z	P_{FDR}
	63 −33 −18	5	3.22	n.s.
Left anterior insula	−36 30 6	9	3.21	n.s.
Left limen insula	−27 12 −18	5	3.17	n.s.
Right anterior orbital gyrus	24 48 −9	6	3.17	n.s.
Left IPS	−51 −45 48	5	3.14	n.s.
Precuneus	15 −72 21	5	3.11	n.s.
Left inferior frontal gyrus	−51 36 15	10	3.09	n.s.
Left lateral orbitofrontal gyrus	48 36 −12	6	3.07	n.s.
Cerebellum	−9 −75 −33	10	3.04	n.s.
Left IPS	−24 −63 39	15	2.99	n.s.
Pulvinar	12 −33 9	5	2.91	n.s.
Anterior cingulate cortex	6 −21 36	7	2.87	n.s.
VS	−12 3 6	5	2.83	n.s.

[a] Italics indicate that a peak falls under the same cluster as the preceding peak

[b] Cluster size in voxels

[c] Significant at $P_{FDRcorrected} = 0.05$ across the whole brain

[d] Significant at $P_{FDRcorrected} = 0.05$ across the ROIs

Table 5

Significant peaks of UnTless − ExpTless

Area	*x, y, z* MNI[a]	K[b]	Z	P_{FDR}
Left anterior insula	−36 18 −6	44	4.47	0.033[c]
Right anterior insula	33 21 0	13	3.9	0.033[c]
Superior frontal gyrus	−9 6 63	48	4.48	n.s.
	0 12 57		2.93	n.s.
Left superior frontal sulcus	−24 −6 60	53	4.25	n.s.
	−18 −12 57		3.95	n.s.
	−30 0 66		2.64	n.s.
Right middle temporal gyrus	66 −30 −6	69	4.06	n.s.
	66 −39 3		3.45	n.s.
	72 −36 −6		3.27	n.s.
Substantia nigra	9 −15 −9	37	3.95	n.s.
Mediodorsal thalamus	12 −12 6	37	3.81	n.s.
	6 −3 3		3.08	n.s.
Superior frontal gyrus	18 −6 69	7	3.76	n.s.
Right cerebellum	18 −66 −30	29	3.76	n.s.
	9 −69 −24		3.48	n.s.
Superior frontal gyrus	6 36 51	21	3.73	n.s.
	0 42 45		2.78	n.s.
Superior precentral sulcus	−39 0 42	44	3.51	n.s.
Left cerebellum	−21 −63 −33	7	3.48	n.s.
Substantia nigra	−6 −21 −9	8	3.47	n.s.
Left middle temporal gyrus	−54 −33 −12	10	3.43	n.s.
Superior frontal gyrus	−12 −24 69	5	3.41	n.s.
Inferior frontal sulcus	−54 21 15	12	3.36	n.s.
Anterior cingulate cortex	9 27 30	16	3.24	n.s.
Anterior cingulate cortex	−6 33 3	11	3.21	n.s.
Cerebellum	−9 −69 −27	6	3.19	n.s.
Pulvinar	15 −36 0	5	3.18	n.s.
Right inferior frontal gyrus	45 18 24	6	3.13	n.s.
Superior frontal gyrus	−15 12 48	5	3.08	n.s.
Middle frontal gyrus	54 −3 42	7	3.06	n.s.
Superior temporal gyrus	51 −45 9	5	3.00	n.s.
	−9 −3 6	6	2.96	n.s.
Left VS	−15 3 −3	14	2.90	n.s.
Cerebellum	33 −60 −30	5	2.86	n.s.
Cuneus	15 −87 9	5	2.85	n.s.
Anterior cingulate cortex	9 36 3	6	2.85	n.s.
Left inferior frontal gyrus	51 12 24	5	2.77	n.s.

[a] Italics indicate that a peak falls under the same cluster as the preceding peak

[b] Cluster size in voxels

[c] Significant at $P_{FDRcorrected} = 0.05$ across the ROIs